19th Brazilian Congress of Thermal Sciences and Engineering
November 6th–10th, 2022, Bento Gonçalves - RS - Brazil

ENC-2022-0098
Laplace Transform-Based Modeling of Heat Transfer in Producing Wellbores

Eduardo Bader Dalfovo Mohr Alves
Arthur Pandolfo da Veiga
André de Souza Matos Vicente
Jader Riso Barbosa Jr.
Departamento de Engenharia Mecânica, Universidade Federal de Santa Catarina, Florianópolis, SC, 88040-900, Brazil
eduardo.alves@polo.ufsc.br
arthur.pandolfo@polo.ufsc.br
andre.vicente@polo.ufsc.br
jrb@polo.ufsc.br

Abstract. *This paper presents a novel, consistent approach to model heat transfer in hydrocarbon producing wells to simulate Annular Pressure Buildup (APB) in offshore wells. The modeling framework is built on a state-of-the-art APB simulator and complements traditional (i.e., pseudo-steady-state) models by including terms initially neglected in transient simulators. To achieve that, a formulation based on the Laplace transformation of the governing differential equations is constructed and solved in the transformed space. The main objective of applying the transformation is to propose a better-suited formulation to simulate shorter timespans. Data gathered from an actual oil-producing well validate the method, leading to two main sets of results. The first is a comparison against field data for temperature and pressure in the production line at the wellhead. In such a study, it is expected that the new Laplace-based model adjusted better to the actual field data. In the second study, the main result is a comparison of the APB in each annuli using the pseudo-steady-state simulator and the new Laplace model. Due to the better representation of the wellhead temperature, the slower warming of the annulus indicates that traditional models overpredicts APB, which could lead to excessive investments in safety factors in the construction of the wellbore. These statements are confirmed with preliminary tests, where a predicted difference of 8* MPa *in the first annulus between the models indicates the importance of using this new heat transfer formulation to simulate the temperature distribution and the related APB.*

Keywords: *Laplace Transform, Wellbore, Heat Transfer, Petroleum Production, APB*

1. Introduction

Correct simulation of the temperature profile during production operations in hydrocarbon producing wells is crucial for properly designing the wellbore structure. When production starts, hot reservoir fluids flow through the production string, exchanging heat with the surrounding rock formation. The temperature difference is due to the geothermal gradient in the earth's crust with an average value of 25 Kelvin per kilometer drilled (Renner, 2007). However, as a consequence of the drilling process, in every wellbore there are fluids trapped in the annular spaces between casings and other tubing. Therefore, as the heat flows outward from the production stream, the temperature of the annular fluids increase, causing their expansion and, consequently, pressure increase. The *Annular Pressure Buildup* (APB), if not taken into account during the design of the wellbore structure, can lead to collapse of the structure and premature end of the well's life cycle (Moe, George Robert; Erpelding, 2000). Many works discussed the risks to the well structure due to wellbore fluid expansion phenomena (Bradford *et al.*, 2004; Ellis *et al.*, 2004; Gosch *et al.*, 2002; Pattillo *et al.*, 2006, 2007) and, as a result, its simulation is highly interesting to the oil industry (Halal and Mitchell, 1994; Oudeman and Bacarreza, 1995; Oudeman and Kerem, 2004; Hasan *et al.*, 2009; Barcelos, 2017; Ferreira *et al.*, 2017).

This paper proposes a novel formulation to accurately predict the wellbore thermal behavior at all stages of oil production. The formulation uses state-of-the-art models to improve the predictions at earlier times by including thermal capacitance terms in the radial heat transfer model, which are usually omitted in more traditional approaches (da Veiga *et al.*, 2022).

2. Methodology

To introduce the problem geometry, Figure 1 presents the general structure of a well completed with three annuli; two are filled with drilling mud/completion fluid and the other is cemented up to the wellhead.

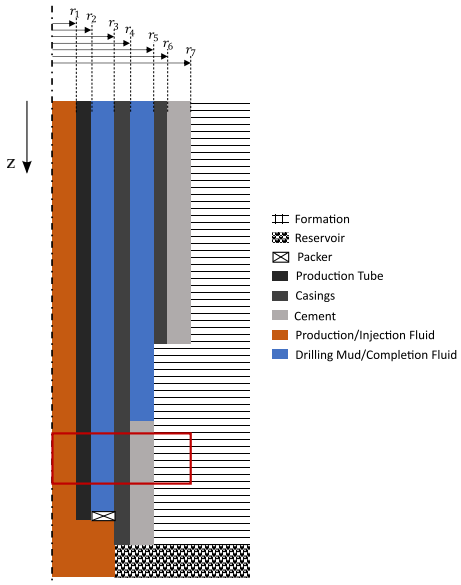

Figure 1. Schematic diagram of a generic well with two annuli filled with packer fluids and one annulus cemented up to the wellhead. r_1 to r_7 are the radii of the interfaces between different materials/domains. The rectangular region (red contour) near the bottom of the well is used to illustrate the derivation of the model equations.

The thermal problem consists of a set of differential equations which are integrated along the well. The equations are split between the production fluid (two-phase momentum and energy balances) and the sealed annuli, in which mass conservation and the hydrostatic pressure relationships are solved.

By disregarding the transient and kinetic energy terms in the momentum and energy balances, and the heat conduction in the axial direction in the energy equation, the conservation equations for the production stream assume a pseudo-steady-state form as follows da Veiga *et al.* (2022):

$$\frac{\partial P}{\partial z} = -\frac{f_S \rho_{ns} v_m}{2 d_T} + \rho_s \sin(\theta) \tag{1}$$

$$\frac{\partial h}{\partial z} = \frac{Q'}{\dot{m}} - g \sin(\theta) \tag{2}$$

where P is the pressure, f_s is the two-phase friction factor (with slip), ρ_{ns} is the non-slip fluid density at the local P and T, v_m is the mixture velocity, d_T is the inner diameter of the production tubing. To calculate the values of f_s and ρ_s, the Beggs and Brill (1973) correlations were used with the corrections of Brill and Beggs (1991). h is the enthalpy of the produced fluid, $\dot{m}$ is the mass flux, g is the acceleration of gravity, θ is the inclination from the horizontal and Q' is the the heat flow per unit length. In both equations, z is the wellbore length. As most wells deviate from the vertical, the integration path follows the curvature of the well.

For each annulus the sets of differential equations are given by:

$$\frac{\partial P}{\partial z} = g \sin(\theta) \tag{3}$$

$$\frac{\partial M}{\partial z} = \pi \rho \left(r_{out}^2 - r_{inn}^2 \right) \tag{4}$$

where r_{out} and r_{inn} represent the local outer and inner annulus radii. Note that by writing the mass conservation in this format, it is possible to couple structural deformation models with the effects of fluid expansion due to heating by taking into account the radial displacement of the casings.

In order to calculate the local density of the packer fluids, one must first know the local pressure and temperature. Although the former is obtained by integrating Eq. 3, the latter is calculated from an equivalent thermal network that determines the heat flow per unit length used in Eq. 2. Thus, at each depth, a equivalent thermal network is assembled

Figure 2. Equivalent resistances and capacitances of the thermal network.

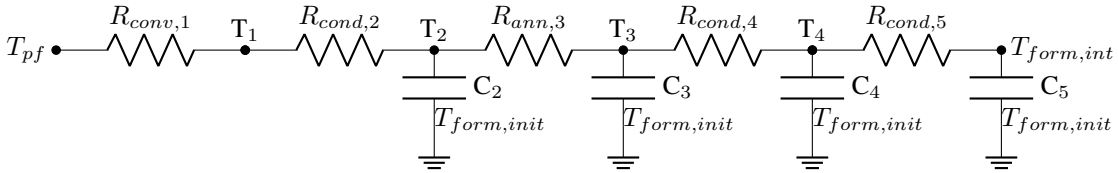

considering the thermal capacitances of the materials (casings, trapped fluids and cement), as shown in Fig. 2, which illustrates the thermal network for the highlighted region in Fig. 1.

In Fig. 2, the subscripts indicate which interface is used to calculate the temperatures and the heat flux. For example, T_{pf} represents the temperature at the center line of the production stream and T_1 is the temperature at the interface with the production tubing. For the specific geometry presented in Fig. 1, surrounding the production tube there is an annulus filled with packer fluid (between T_2 and T_3), another steel tube (between T_3 and T_4) and a layer of cement in contact with the rock formation.

Due to the comparatively higher magnitude of the heat advection in the production fluid, the capacitance term is omitted at the innermost interface. At each interface, a heat balance through the interface and adding the term stored in the material previous to the node. Mathematically this is written as:

$$C_i \frac{\partial T_i}{\partial t} = Q'_i - Q'_{i+1} \tag{5}$$

where the heat flux at each node is calculated using the thermal resistances:

$$Q'_i = \frac{T_i - T_{i-1}}{R_i} \tag{6}$$

The resistances are computed via heat transfer correlations, which depend on the interface analyzed. For example, for the forced convection in the production fluid, the resistance is calculated with the correlation proposed in Chen (1966). For the case of trapped fluid in the annulus, it is assumed natural convection and the correlation used is of Zhou (2013) with a parallel resistance for radiation between the solids surrounding the fluids, as proposed by Hasan and Kabir (1994). In the solid regions, i.e. cement, tubing and casings, the pure conduction resistance for radial diffusion is used (Incropera *et al.*, 2000, p. 126).

For the outermost node (wellbore interface with the formation), the heat diffusion can be solved coupled with the thermal network. In fact, the last heat term used in Eq. 5 is given by:

$$Q'_{fm} = -2\pi k_{fm}\, r \frac{\partial T_{fm}}{\partial r}\bigg|_{r=r_{fm}} \tag{7}$$

where r_{fm} is the formation inner radius, k_{fm} is the formation thermal conductivity and T_{fm} is the formation temperature.

Traditional approaches, such as those of Ramey (1962); Hasan and Kabir (1991) consider the formation as a semi-infinite medium; this consideration is also made in this paper. However, the inner boundary condition in those papers consider a steady heat flow over time. In the proposed model, a prescribed temperature is assumed. This temperature is the time-dependent temperature at the outermost node of the thermal network. Thus:

$$\begin{cases} \dfrac{\partial^2 T_{fm}}{\partial r^2} + \dfrac{1}{r}\dfrac{\partial T_{fm}}{\partial r} = \dfrac{1}{\alpha_{fm}}\dfrac{\partial T_{fm}}{\partial t} & (8) \\ T_{fm}(r, t=0) = T_{init} & (9) \\ \lim\limits_{r\to\infty} T_{fm}(r,t) = T_{init} & (10) \\ T_{fm}(r = r_{fm}, t) = T_{int} & (11) \end{cases}$$

where the temperature is solved in the formation domain, T_{int} is the temperature at the outermost node of the thermal network and T_{init} is the initial temperature of the boundary value problem, in this case the geothermal temperature. α_{fm} is the thermal diffusivity of the rock formation.

The governing equations are non-dimensionalized in terms of the following dimensionless groups:

$$T_{D,i} = \frac{T_i - T_{init}}{T_{init}} \tag{12}$$

and

$$\tau = \frac{t\alpha_{fm}}{r_{fm}^2} \tag{13}$$

To solve the dimensionless boundary value problem, the Laplace transform is used. This is one of the Integral Transformations which have the characteristic of mapping a function from its original functional space into a transformed version of it, while retaining information of the original function. By transforming the domain studied it is possible to convert Differential Equations into algebraic equations which can be solved with simpler methods. Mainly, when transforming differential equations, it is possible to embed into the transformed expression some boundary conditions, reducing considerably the amount of calculation required to solve the equation (Beerends *et al.*, 2003). The solution in the Laplace domain is given by:

$$\overline{T}_D(r_D, s) = \frac{\overline{T}_{D,int} K_0(r_D\sqrt{s})}{K_0(\sqrt{s})} \tag{14}$$

where r_D is the dimensionless radius, $\overline{T}_D$ is the dimensionless temperature in the Laplace domain and s is the time variable transformed into the Laplace domain. K_0 is the modified Bessel function of the second kind and order 0.

Now, by applying the Laplace transform in every nodal equation it is possible to re-write the sets of differential equations to a simple linear system to be solved in the Laplace domain. This is given by:

$$\begin{cases} \overline{T}_{D,i} = \dfrac{T_{D,pf}}{s}, & \text{i=0} \quad (15) \\ (R_i + R_{i+1})\overline{T}_{D,i} - R_i\overline{T}_{D,i+1} - R_{i+1}\overline{T}_{D,i-1} = 0 & \text{i=1} \quad (16) \\ \left[R_i C_i \dfrac{\alpha_{fm}}{r_{fm}^2} s + \dfrac{2\pi k_{fm} R_i \sqrt{s} K_1(\sqrt{s})}{K_0(\sqrt{s})} + 1\right]\overline{T}_{D,i} - \overline{T}_{D,i-1} = 0 & \text{i=int} \quad (17) \\ \left(R_i R_{i+1} C_i \dfrac{\alpha_{fm}}{r_{fm}^2} s + R_i + R_{i+1}\right)\overline{T}_{D,i} - R_i\overline{T}_{D,i+1} - R_{i+1}\overline{T}_{D,i-1} = 0 & \text{otherwise} \quad (18) \end{cases}$$

This system of equations can be solved by a simple inversion of the coefficient matrix for a set of values of s in the Laplace domain. To return the solution to the real time domain, it is possible to use numerical inversion techniques. In this paper, the Concentrated Matrix Exponential (CME) method (Horváth *et al.*, 2020) was used. This is a method based in the framework of the Abate-Whitt family of numerical inversion (Abate and Whitt, 2006). Many methods exists within this framework, however, the CME provides more versatility in the inversion step. For example, the Stehfest (1970) algorithm is usually faster, but limited to a small number of inversion nodes. The CME provides hundreds of inversion nodes increasing the chance of finding the converged solution.

The next step involves computing thermo-elastic deformations associated with each casing, tubing, cement or even the formation itself. In this paper, the same formulation presented by da Veiga *et al.* (2022) was used, based on the model of Halal and Mitchell (1994). In this formulation, an axyssimetric formulation is used for the plane deformation at each deformation node. The advantage of using this model is the simplicity to couple it with the integration procedure and to have a consistent formulation that grants continuity of stress and deformation even for multiple solids in contact.

This set of equations is solved at each point of the longitudinal integration procedure. Once the entire wellbore is solved, the total mass of each annulus is is obtained from the solution of Eq. 4 and it is possible to compare it with its initial mass. The difference in the result is used to create a residue equation that can be iteratively solved to find the correct pressurization of each annulus. The procedure for such is to change the initial condition for the pressure in each annulus (Eq. 3) until the mass after the heating is equal to the initial mass of the system. To solve this problem, a multidimensional root finder is used.

For the initial conditions of the production tube, the pressure and temperature of the produced fluid is given at the depth of the Permanent Downhole Gauge (PDG). In each annulus, for the differential equations for the mass, at the bottom the mass is set to zero, such that by integrating along the wellbore this computes the mass of each annulus.

In order to calculate the properties of the produced fluid and all annular trapped fluids, a set of thermodynamic property tables is generated using appropriate models (INFOCHEM/KBC, 2019). These tables are then interpolated based a the thermodynamic state known at each point. For the production fluid it is a pair of pressure and enthalpy. Meanwhile, for the annular fluid, a pair of pressure and temperature is used and single phase of liquid is assumed.

2.1 Considerations about pseudo-steady-state formulations

It is easy to check that the Laplace based approach actually reproduces the traditional pseudo steady-state formulation for sufficiently long times. The first step consists of evaluating the behavior of Eq. 5 in the large time limit, which leads

to small variations in the temperature time derivative. When that occurs, the heat balance at each interface is given by the thermal network formed only by the resistance terms. In mathematical form, the heat balance at any interface is given by:

$$(R_i + R_{i+1})T_i - R_i T_{i+1} - R_{i+1} T_{i-1} = 0 \tag{19}$$

This balance is used in every node, except the one in contact with the formation. However, since the derivative of the temperature with respect of time in the last node is approximately null, the heat equation in the formation falls in the same behavior as is the result of steady heat flow.

The solution for the heat flow entering the formation for this condition is given by:

$$\overline{Q}'_D = \frac{K_1(\sqrt{s})}{\sqrt{s}K_0(\sqrt{s})} \tag{20}$$

As this solution does not have an analytical inversion, many authors propose approximation functions in order to estimate the term. These are the time-functions presented in several works (Hasan and Kabir, 1994; Hagoort, 2004; Ferreira, 2017).

In this paper, for the comparison between the new model and the traditional pseudo steady-state approach, the time function of Hasan and Kabir (1991) was used, as the literature states that this is a good approximation for long term operations.

3. Results and Discussions

To validate the heat transfer model, a real well geometry is used to compare the results with field data obtained during an extended well test, which means that the well is producing for the first time in its entire life cycle. Generally, oil wells are more heavily instrumented in such tests, yielding a higher degree of confidence in the field data. In this paper, the data used is provided by the well's operator, and is presented without previous treatment. The measurements are performed directly in the field, with standard industry gauges and measurement tools.

Figure 3 presents the wellbore geometry and fluids trapped in each annulus. According to the well operator, the rock formation surrounding the well is composed mainly of shale. In this geometry there are three annuli which will be heated by the production. Due to the limited information about the type of fluid filling each annular space (only their densities are known) it is assumed a composition similar to pure brines (based on NaCl) with different concentrations. The amount of salt added to each composition is such to match the density of the fluid at the standard condition.

In the figure, it is also possible to see the depth of the PDG and TPT, both contain sensor from which the data for pressure and temperature are taken both for use as the initial condition, of the marching problem, and as for comparison with the simulated profiles in the wellhead.

Although the deviation is not large, at the production depth the drilling occurred at an angle of approximately 20°. The *kick-off* point for the deviation occurred at 4909 meters.

The well has a total depth of 5857.16 m, with a measured temperature of 375.15 K as a consequence of the geothermal gradient. The seadepth is 2051 m and the temperature of the seabed is 277.15 K.

As for the inputs to the simulation, Fig. 4 presents a graphical representation of measured flow rate, pressure and temperature of this well during the test. The start of the production is set as the reference time for every simulation. There is a total of two production intervals the first one ending just after 15 days of production, then there is a brief shut down interval that ends at 17 days. The second production interval has a greater production rate and ends just after the start of the 28th day of production. This is the raw data as provided for this paper, which have some problems related to synchronization of each measured variable.

A first treatment was performed before using the data in the models, initially a small lag was perceived from the PDG data and the measurement of flow rate at the platform. In order to correct the timing of the variables, an automatic cross correlation scheme was used to sync the flow rate reading and the data at the PDG. A lag of 28 minutes was added to the PDG data in order to achieve maximum correlation. The automatic procedure used a smoothing by means of a convolution of the data and the Bohman window (Harris, 1978) and the correlation was determined with the filtered data (Ifeachor and Jervis, 1993).

However, even with the lag added, a 12 hour window was not accounted in the flow rate measurement. Reasons for this lack of data could be related to the filling of the production line, production separator or even problems in the flow rate measurement. As a consequence, a extrapolation of the initial values measured for the flow rate is assumed during the first 3 hours of production.

Another data treatment performed involves using the average flowrate. The reason of why this procedure is done is related to the nature of both models. As the hydrodynamic problem does not contain transient terms, using the instantaneous flowrate values, the formulation would assume that the instant value would affect the production during the entire flow duration. Thus, by using the cumulative average, it is possible to vary the flowrate input, without removing entirely the effects of flow variation in time.

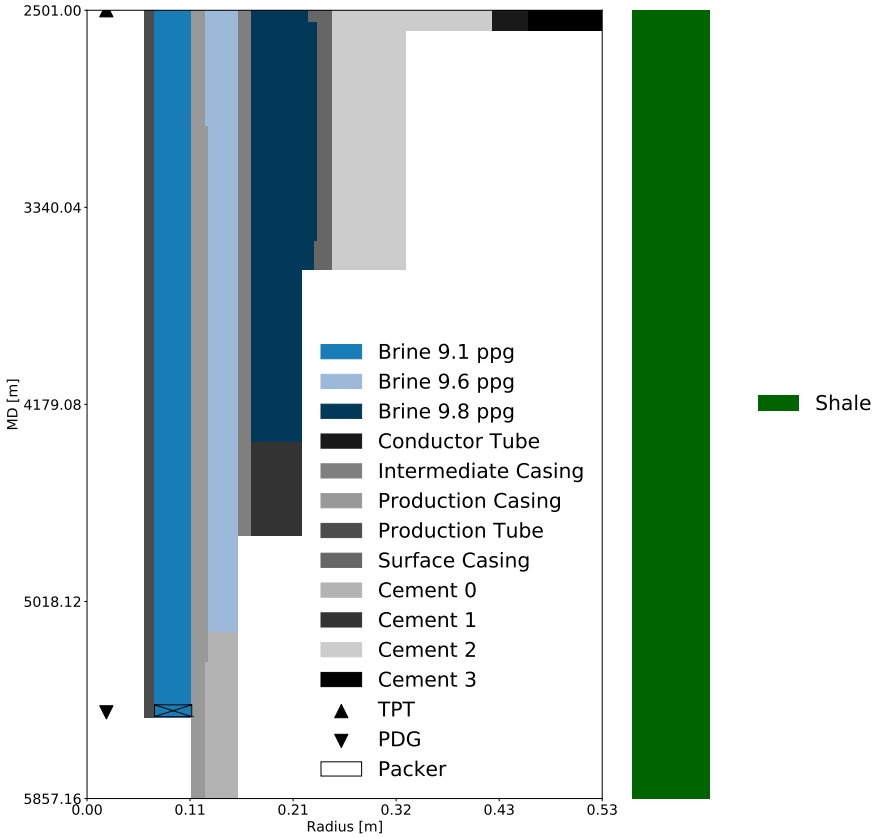

Figure 3. Schematic geometry of the studied well. Gray scale colors indicate solid materials as described in the legend. Blue tones indicates the presence of trapped fluid in each annulus. The rightmost green bar is the formation lithology, in this case pure shale.

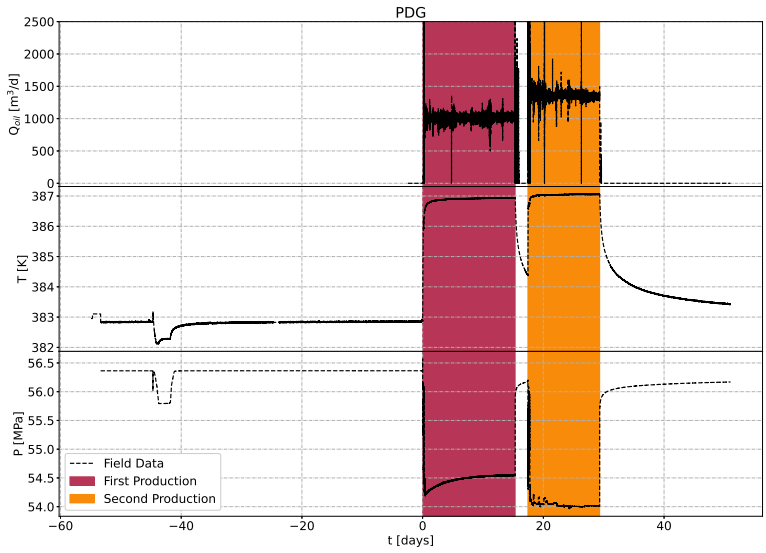

Figure 4. Raw inputs for the hydrodynamic model in the well during EWT. The top plot shows the oil flow rate at the topside. The middle plot is the pressure at the PDG and the last one is temperature. Red region represents the first production interval meanwhile the yellow region is the second production interval.

Since the formulation does not involve a marching procedure with respect to time, the number of points used in the simulation does not affect the final result. Fig. 5 presents the inputs used in the simulation. For validation, from the start, a set of points were taken every 15 minutes up to 6 hours. At this point, the time spacing was increased to 6 hours until

the end of the first production interval, in 15 days. As the second interval occurs after a well shut-down, the models are expected to perform poorly. Therefore less points are taken in this interval. In total, 104 points were used.

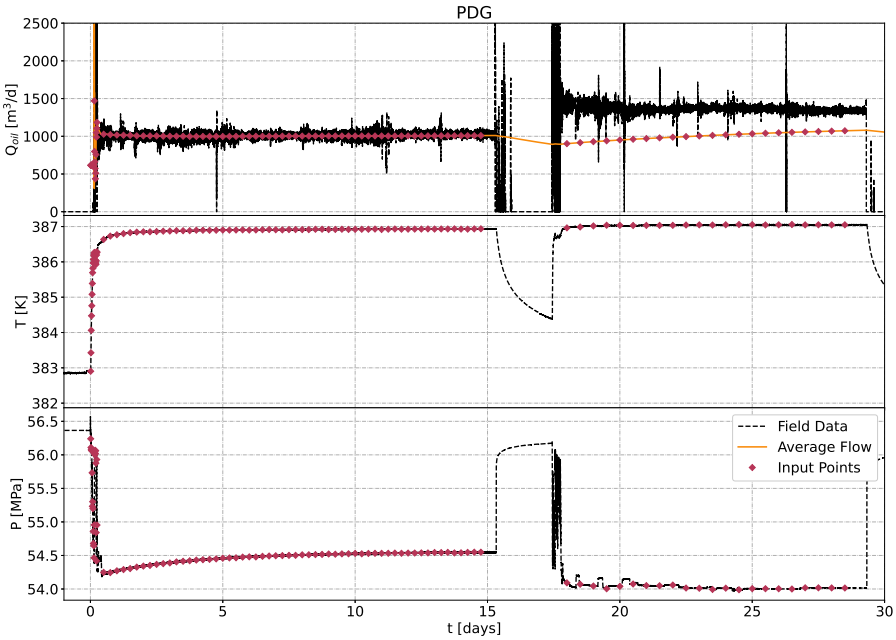

Figure 5. Inputs for the hydrodynamic problem. Red dots marks the values used as the initial condition for the marching scheme. For the flow rate the cumulative average is used.

In Fig. 6, the temperature and pressure at the wellhead are presented with the field data registered at the TPT. Both methods achieved good results. However, there are three main regions which can be analysed independently. After the first 12 hours of production, and prior to 15 days, both models agreed accurately with the field data. Especially after the first day, the Hybrid-Laplace model managed to outperform the traditional pseudo steady-state method. This behavior, however, changes by the end of the first production interval, when the Laplace model tends to over-predict the wellhead temperate. Although this may seem detrimental to the model, the difference is less than 1 K, which is within the the uncertainty of the field data. Similar to a vertical well vertical well simulated by Alves *et al.* (2021), the difference in predicted pressure appears to be an small offset in relation to the field data, indicating imprecision in the two-phase flow correlation used.

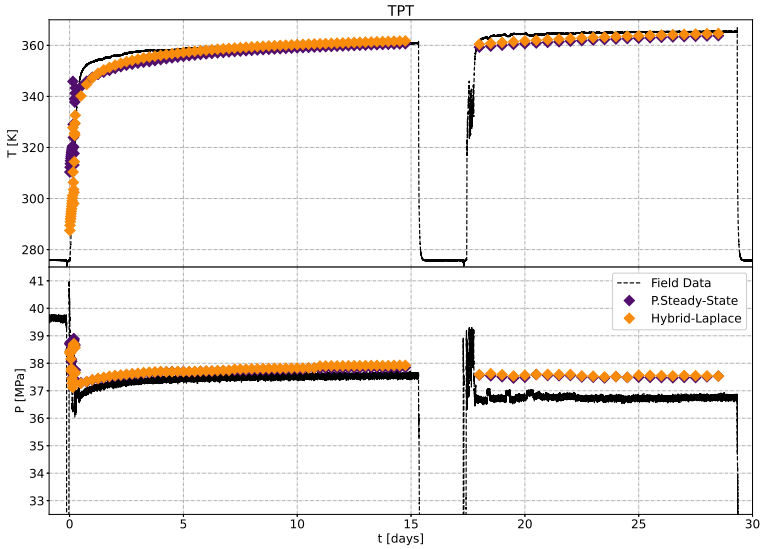

Figure 6. TPT comparison from different models and the field data. The purple diamonds are results of the simulation using the traditional pseudo steady-state as presented in da Veiga *et al.* (2022). The yellow diamonds are results from the hybrid-Laplace formulation.

To confirm that the the Laplace model captures more information during the start of production, Fig.7 zooms to the first 12 hours of production. As mentioned previously, in the first 3 hours of production the flow rate is extrapolated to a single value. This is noticed at the start of the production in the region where both models follow a common behavior. The largest deviations from the field data, with regard to temperature, occurs in the first two hours. In this region, a maximum deviation of 13.38 K for the Hybrid-Laplace model and 35.68 K for the pseudo steady-state model is perceived. Again, a simple explanation for this deviation is the lack of flow information, which is further confirmed by the fact that in regions where the flow measurement is more reliable, the predictions achieved better precision.

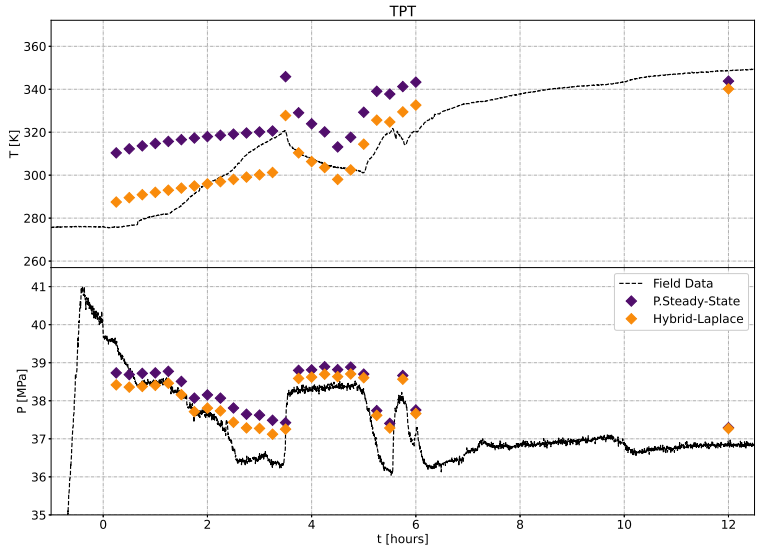

Figure 7. TPT comparison from different models and the field data with focus in the start of the first production interval. Same coloring scheme is used from previous figure.

This figure is a good indicator that the Laplace model better captures the trend of the data. In fact, from the interval after the flow data started to be measured and, not extrapolated, up to the first 5 hours of production the maximum deviation detected for the Laplace model was of 2 K, whereas the pseudo steady-state formulation had an average deviation of 3.68 K in the same region.

Taking the data from Fig.6, the absolute average deviation (AAD) for both temperature and pressure was analyzed considering the two models. For the pressure, almost no perceptible difference was detected, as both the Laplace model and the pseudo steady-state have AAD of 1.3%. However, for the wellhead temperature, the Laplace model has an AAD of 0.9% against 2.2% for the pseudo steady-state. This information, in the context already presented that the Laplace model matches the pseudo steady-state for long operations, confirms that both models are suited to predict the heat transfer in oil wells, with the Laplace model achieving better results for shorter term operations.

Figure 8 presents the behavior of the APB in each annulus along the production intervals. It is important to explain that the APB, is defined as the maximum value of the pressure variation in each annulus. As expected, at the start of the production, before the first day, due to the slower heat transfer to the annuli, the APB is less pronounced with the Laplace formulation. In fact, for annulus B, the first predicted APB is 2.80 MPa and for annulus C it is 0.76 MPa. Meanwhile, the pseudo steady-state predicts APBs of the order of 18.71 MPa in annulus B and 14.65 MPa in annulus C. This difference actually settles after the first day of production, when the heat transfer from both models converges to the nearest value. After this point, a small deviation occurs due to the nature of the Laplace model, which predicts higher temperatures for the fluids, but at the end of the second production interval there is no significant difference in the APB for annulus A and B. For annulus C, the furthest from the center line of the well, because it is being heated, large difference is observed.

4. Conclusion

This paper proposed a new formulation to predict the heat transfer in hydrocarbon production wells. This formulation is implemented in conjunction with a state-of-the-art simulator with the intention to understand the behavior of the APB during short-time operations. To validate the proposed model, field data taken from an actual wellbore was used and confirmed the capacity of the formulation to better represent the heat transfer in shorter times, while keeping the capacity to reproduce the behavior of traditional formulation at longer times. It was detected that this formulation does not only impact the heat transfer dynamic, but also changes the rate of increase of the APB in each annulus non-uniformly.

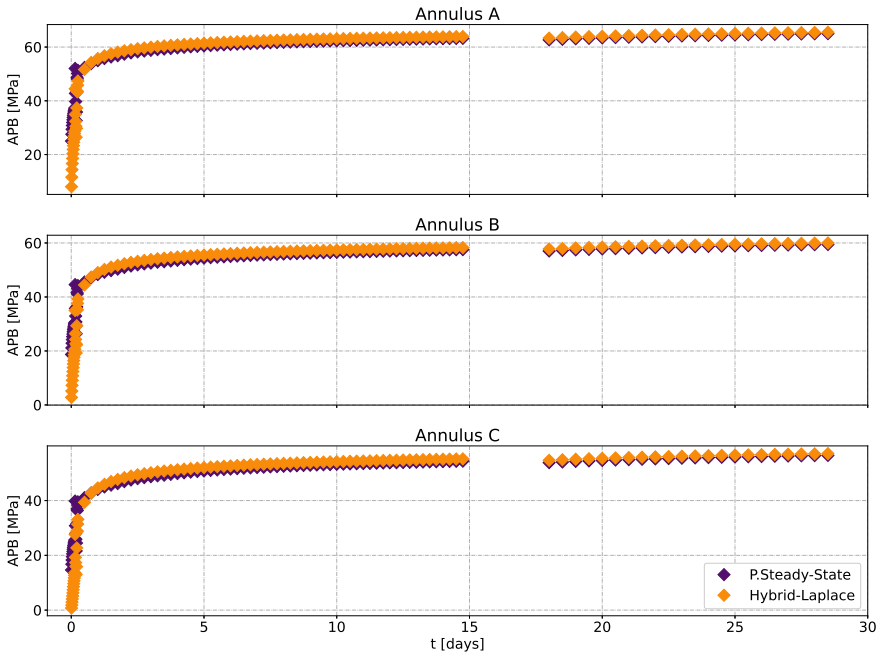

Figure 8. Predicted APB in each annulus during both production intervals. Top plot is related to the first annulus (A), meanwhile the middle is related to the second (B) and the bottom to the third (C). The darker diamonds are referring to the pseudo steady-state formulation, meanwhile the brighter one is with the Laplace formulation.

5. REFERENCES

Abate, J. and Whitt, W., 2006. "A unified framework for numerically inverting laplace transforms". *INFORMS Journal on Computing*, Vol. 18, No. 4, pp. 408–421. ISSN 10919856. doi:10.1287/ijoc.1050.0137.

Alves, E.B.D.M. *et al.*, 2021. "Coupled modeling of heat transfer and deformation of salt layers in hydrocarbon producing wells".

Barcelos, J.G.A., 2017. *Modelagem Matemática do Aumento de Pressão nos Anulares (APB) em Poços de Petróleo*. Ph.D. thesis, Universidade Federal de Santa Catarina.

Beerends, R.J., ter Morsche, H.G., van den Berg, J.C. and van de Vrie, E.M., 2003. *Fourier and laplace transforms*. Cambridge University Press. ISBN 9780521806893.

Beggs, H.D. and Brill, J.P., 1973. "A Study of Two-phase Flow in Inclined Pipes". *Journal of Petroleum Technology*, p. 10. doi:10.2118/4007-pa.

Bradford, D., Fritchie, D., Gibson, D., Gosch, S., Pattillo, P., Sharp, J. and Taylor, C., 2004. "Marlin Failure Analysis and Redesign: Part 1 - Description of Failure". *SPE Drilling & Completion*, Vol. 19, No. 02, pp. 104–111. ISSN 1064-6671. doi:10.2118/88814-pa.

Brill, J.P. and Beggs, H.D., 1991. *Two-Phase Flow in Pipes, 6th Edition*.

Chen, J.C., 1966. "Correlation for boiling heat transfer to saturated fluids in convective flow". *Industrial and Engineering Chemistry Process Design and Development*, Vol. 5, No. 3, pp. 322–329. ISSN 01964305. doi:10.1021/i260019a023.

da Veiga, A.P., Martins, I.O., Barcelos, J.G., Ferreira, M.V.D., Alves, E.B., da Silva, A.K., Hasan, A.R. and Barbosa, J.R., 2022. "Predicting thermal expansion pressure buildup in a deepwater oil well with an annulus partially filled with nitrogen". doi:https://doi.org/10.1016/j.petrol.2021.109275.

Ellis, R., Fritchie, D., Gibson, D., Gosch, S. and Pattillo, P., 2004. "Marlin Failure Analysis and Redesign: Part 2 - Redesign". *SPE Drilling & Completion*, Vol. 19, No. 02, pp. 112–119. ISSN 1064-6671. doi:10.2118/88838-pa.

Ferreira, M.V., Hafemann, T.E., Barbosa, J.R., da Silva, A.K. and Hasan, R., 2017. "A numerical study on the thermal behavior of wellbores". *SPE Production & Operations*, Vol. 32, No. 04, pp. 564–574.

Ferreira, M.V.D., 2017. *Estudo Termo-Estrutural de Poços Equipados com Tubos Isolados a Vácuo*. Ph.D. thesis, Universidade Federal de Santa Catarina.

Gosch, S., Horne, D., Pattillo, P., Sharp, J., Shah, P. *et al.*, 2002. "Marlin failure analysis and redesign; part 3, vit completion with real-time monitoring". In *IADC/SPE Drilling Conference*. Society of Petroleum Engineers.

Hagoort, J., 2004. "Ramey's Wellbore heat transmission revisited". *SPE Journal*, Vol. 9, No. 4, pp. 465–474. ISSN 1086055X. doi:10.2118/87305-PA.

Halal, A. and Mitchell, R., 1994. "Casing Design for Trapped Annular Pressure Buildup". *SPE Drilling & Completion*,

Vol. 9, No. 02, pp. 107–114. ISSN 1064-6671. doi:10.2118/25694-pa.

Harris, F.I., 1978. "On the use of windows for harmonic analysis with the discrete Fourier transform". *Proceedings of the IEEE*, Vol. 66, No. 1, pp. 51–83. ISSN 0018-9219. doi:10.1109/PROC.1978.10837.

Hasan, A.R., Izgec, B. and Kabir, C.S., 2009. "Ensuring sustained production by managing annular-pressure buildup". *Society of Petroleum Engineers - EUROPEC/EAGE Conference and Exhibition 2009*, , No. 1994. doi:10.2118/121754-ms.

Hasan, A.R. and Kabir, C.S., 1991. "Heat Transfer During Two-Phase Flow in Wellbores; Part I–Formation Temperature". pp. 469–478. doi:10.2118/22866-ms.

Hasan, A.R. and Kabir, C.S., 1994. "Aspects of Wellbore Heat Transfer During Two-Phase Flow". *SPE Production & Facilities*, , No. August.

Horváth, G., Horváth, I., Almousa, S.A.D. and Telek, M., 2020. "Numerical inverse Laplace transformation using concentrated matrix exponential distributions". *Performance Evaluation*, Vol. 137, p. 102067. ISSN 01665316. doi:10.1016/j.peva.2019.102067.

Ifeachor, E.C. and Jervis, B.W., 1993. *Digital Signal Processing*. ISBN : 0-201- 54413-X.

Incropera, F.P., Dewitt, D.P. and Bergman, T.L., 2000. *Fundamentos de Transferência de Calor E de Massa* . Grupo Gen-LTC.

INFOCHEM/KBC, 2019. "Multiflash™".

Moe, George Robert; Erpelding, P., 2000. "Annular Pressure Buildup: What it is and what to do about it."

Oudeman, P. and Bacarreza, L.J., 1995. "Field Trial Results of Annular Pressure Behavior in a High-Pressure/High-Temperature Well". *SPE Drilling & Completion*.

Oudeman, P. and Kerem, M., 2004. "Transient Behavior of Annular Pressure Build-up in HP / HT Wells". *International Petroleum Exhibition and Conference*.

Pattillo, P.D., Cocales, B.W. and Morey, S.C., 2006. "Analysis of an Annular Pressure Buildup Failure During Drill Ahead". *SPE Drilling & Completion*, Vol. 21, No. 04, pp. 242–247. ISSN 1064-6671. doi:10.2118/89775-pa.

Pattillo, P.D., Sathuvalli, U.B.R., Rahman, S.M., Prewett, H.H., Carmichael, S.P., Wydrinski, R. *et al.*, 2007. "Mad dog slot w1 tubing deformation failure analysis". In *SPE Annual Technical Conference and Exhibition*. Society of Petroleum Engineers.

Ramey, H., 1962. "Wellbore Heat Transmission". *J. Petrol. Technol.*, Vol. 14, No. 4, pp. 427–435.

Renner, J., 2007. *Volume VI–Emerging and Peripheral Technologies*.

Stehfest, H., 1970. "Algorithm 368: Numerical inversion of Laplace transforms [D5]". *Communications of the ACM*, Vol. 13, No. 1, pp. 47–49. ISSN 00010782. doi:10.1145/361953.361969.

Zhou, F., 2013. *Research on heat transfer in geothermal wellbore and surroundings*. Doctoral thesis, Technische Universität Berlin, Fakultät VI - Planen Bauen Umwelt, Berlin. doi:10.14279/depositonce-3861.

6. RESPONSIBILITY NOTICE

The authors are solely responsible for the printed material included in this paper.